https://doi.org/10.5607/en.2017.26.5.295
Exp Neurobiol. 2017 Oct;26(5):295-306.
pISSN 1226-2560 • eISSN 2093-8144

Original Article

Experimental Neurobiology

Check for updates

Inhibition of HIF1α and PDK Induces Cell Death of Glioblastoma Multiforme

Jiwon Esther Han[1], Pyung Won Lim[1], Chul Min Na[1], You Sik Choi[1], Joo Young Lee[1], Yona Kim[1], Hyung Woo Park[1], Hyo Eun Moon[1], Man Seung Heo[2], Hye Ran Park[1], Dong Gyu Kim[1] and Sun Ha Paek[1,3,4]*

[1]Department of Neurosurgery, Seoul National University College of Medicine, Seoul 03082,
[2]Smart Healthcare Medical Device Research Center, Samsung Medical Center, Seoul 06351,
[3]Cancer Research Institute, Seoul National University College of Medicine, Seoul 03082,
[4]Hypoxia Ischemia Disease Institute, Seoul National University College of Medicine, Seoul 03082, Korea

Glioblastoma multiforme (GBM) is the most common and aggressive form of brain tumors. GBMs, like other tumors, rely relatively less on mitochondrial oxidative phosphorylation (OXPHOS) and utilize more aerobic glycolysis, and this metabolic shift becomes augmented under hypoxia. In the present study, we investigated the physiological significance of altered glucose metabolism and hypoxic adaptation in the GBM cell line U251 and two newly established primary GBMs (GBM28 and GBM37). We found that these three GBMs exhibited differential growth rates under hypoxia compared to those under normoxia. Under normoxia, the basal expressions of HIF1α and the glycolysis-associated genes, PDK1, PDK3, and GLUT1, were relatively low in U251 and GBM28, while their basal expressions were high in GBM37. Under hypoxia, the expressions of these genes were enhanced further in all three GBMs. Treatment with dichloroacetate (DCA), an inhibitor of pyruvate dehydrogenase kinase (PDK), induced cell death in GBM28 and GBM37 maintained under normoxia, whereas DCA effects disappeared under hypoxia, suggesting that hypoxic adaptation dominated DCA effects in these GBMs. In contrast, the inhibition of HIF1α with chrysin suppressed the expression of PDK1, PDK3, and GLUT1 and markedly promoted cell death of all GBMs under both normoxia and hypoxia. Interestingly, however, GBMs treated with chrysin under hypoxia still sustained higher viability than those under normoxia, and chrysin and DCA co-treatment was unable to eliminate this hypoxia-dependent resistance. Together, these results suggest that hypoxic adaptation is critical for maintaining viability of GBMs, and targeting hypoxic adaptation can be an important treatment option for GBMs.

Key words: Glioblastoma, HIF1alpha, hypoxia

INTRODUCTION

Glioblastoma multiforme (GBM) is the most frequent and aggressive subtype of primary brain tumors [1, 2]. Current standard of care for GBMs includes the surgical resection of the primary tumor followed by radiotherapy and chemotherapy [3, 4]. In spite of these multimodal therapeutic interventions, the overall survival period of GBM patients is, on average, only 12~15 months due

Received August 30, 2017, Revised October 7, 2017,
Accepted October 12, 2017

*To whom correspondence should be addressed.
TEL: 82-2-744-8459, FAX: 82-2-2072-3993
e-mail: paeksh@snu.ac.kr

to tumor recurrence [5]. In fact, recurrent GBMs are repopulated with more malignant cells that are resistant to radio- and chemotherapy [6]. Thus, more efficient therapeutic strategies targeting cellular features of GBMs should be developed.

GBMs, like other tumors, utilize a reprogrammed energy metabolism employing reduced mitochondrial oxidative phosphorylation (OXPHOS) and concomitantly increased aerobic glycolysis [7, 8]. Although this metabolic shift, known as the Warburg Effect, is less efficient for generating ATP per unit glucose than mitochondrial OXPHOS, it is adopted by GBMs presumably because it rapidly supplies biosynthetic precursors, circumvents excess production of reactive oxygen species (ROS) in mitochondria, and decreases apoptotic risks of tumor cells [9]. In addition, increased aerobic glycolysis provides acidic extracellular microenvironment, giving a survival advantage to tumor cells over normal cells [10].

Numerous investigations have been carried out to intervene increased aerobic glycolysis in tumor cells [7, 8, 11, 12]. One such strategy is the use of dichloroacetate (DCA), a pyruvate mimetic that inhibits pyruvate dehydrogenase kinase (PDK), which is a negative regulator of pyruvate dehydrogenase (PDH) and blocks the conversions of pyruvate into acetyl-CoA [13]. In fact, the expression levels of PDK isoforms are elevated in various types of tumors, and the administration of DCA offers improved prognosis of certain GBMs and other tumors by reducing aerobic glycolysis [12, 14-17]. Although increased aerobic glycolysis is an important feature of GBMs, studying glycolytic adaptation only in normoxic condition (20% oxygen) might be insufficient to fully understand the actual physiological responses influencing tumorigenicity.

Hypoxia is a well-known feature of tumor microenvironment [18]. GBMs, like other tumor cells, grow well in hypoxic condition by employing increased expression of hypoxia-inducible factor 1α (HIF1α) [19, 20]. Indeed, HIF1α, together with its partner HIF1β, forms a complex which upregulates expression of almost all enzymes in glycolysis [21]. HIF1α/β also upregulates the expression of genes involved in angiogenesis, survival, and migration, resulting in enhanced metastatic potential and resistance to radiotherapy and chemotherapy [21-24]. Since hypoxic adaptation is important for tumorigenicity [18], an effective strategy for treating GBM needs to be studied under hypoxia [25].

In the present study, we investigated the physiological significance of aerobic glycolytic adaptation and hypoxic adaptation with respect to cell viability of U251, a well-established GBM cell line, and the two primary GBMs, GBM28 (initial tumor) and GBM37 (recurrent tumor), which were derived from the same patient. Cellular responses were examined under hypoxia (approximately 1% oxygen) that recapitulates low oxygen levels of *in vivo* tumor microenvironment, and the results were compared to those obtained under normoxia. We demonstrated that, although hypoxia-dependent resistance was still present in all cell types, the inhibition of HIF1α and PDK with chrysin and DCA, respectively, induced cell death of all three GBMs.

MATERIALS AND METHODS

Glioblastoma cell line and primary glioblastoma cells from a human patient

The human glioblastoma cell line U251 and two primary glioblastoma cells (GBM28 and GBM37) were used in this study. The human glioblastoma U251 was purchased from the American Type Culture Collection (ATCC; Manassas, VA, USA). The primary glioblastoma cells, GBM28 and GBM37, were established from the same human patient who received a standard GBM treatment consisting of concurrent radiotherapy and temozolomide (TMZ) treatment followed by adjuvant TMZ as a primary treatment. GBM28 and GBM37 represented initial and recurrent tumors, respectively. The neural stem cell, NSC10, was used as normal control cell and described previously [26]. These GBM cell line and primary cells were cultured with Dulbecco's modified Eagle's medium containing 10% fetal bovine serum (FBS, Gibco Corp., Grand Island, NY, USA) and 1% antibiotics/antimycotics in a 5% CO_2 incubator at 37°C. Cells were routinely passaged by trypsinization using TrypLE$_{TM}$ (Gibco Corp., Grand Island, NY, USA) every 3~4 days. For the hypoxia treatments, O_2 levels were maintained at 1%, with the residual gas mixture being 94% N_2 and 5% CO_2, as compared to the normoxia experiments, in which O_2 levels were maintained at 20%. The experimental protocol for handling human subjects was reviewed and approved by the Institutional Review Board of Seoul National University Hospital (IRB No. H-1009-025-331).

CCK-8 assay

Each of GBM cells was seeded on a 96-well plate at a density of 3×10^3 cells per well and maintained in a 5% CO_2 incubator with 90% relative humidity at 37°C for 24 h to ensure cell attachment. Subsequently, cells were put in a hypoxia incubator (1% O_2) for 72 h. The control groups were prepared in a normoxia incubator (20% O_2). In every 24 h for 3 consecutive days, the effects of hypoxic and normoxic conditions on cell proliferation were evaluated using the Cell Counting Kit-8 (CCK; Dojindo Molecular Technologies, Kumamoto, Japan). The 10 μl of the CCK solution was added per well and incubated for 2 h. Then, cell proliferation was analyzed according to the manufacturer's instructions by measuring the absorbance of the reaction solution at 450 nm with a Multiscan MS spectrophotometer (Labsystems, Stockholm, Sweden). All experi-

https://doi.org/10.5607/en.2017.26.5.295

ments were conducted in triplicate, and these were repeated 2~3 times.

Semiquantitative reverse transcription-polymerase chain reaction (RT-PCR)

GBM cells were lysed and total RNA was isolated using the RNeasy Mini Kit (Qiagen, Valencia, CA, USA) in accordance to the manufacturer's protocol. Then, cDNA was synthesized from 3 μg of the total RNA extracted using the Superscript III cDNA Synthesis Kit (Invitrogen, Carlsbad, CA, USA). A reverse transcriptase polymerase chain reaction (RT-PCR) was performed and the resulting PCR products were resolved by 1.5% agarose gel electrophoresis. Expression levels of transcripts were quantified using ImageJ (NIH, Bethesda, MD, USA). The primer sequences used in this study were as follows: 5'-GAAAGCGCAAGTCCTCAAAG-3' and 5'-TGGGTAGGAGATGGAGATGC-3' for HIF1α; 5'-CGGATCAGAAACCGACACA-3' and 5'-ACTGAACATTCTGGCTGGTGA-3' for PDK1; 5'-TTAATAAGTCCGCATGGCGC-3' and 5'-TGAAGCATCCCTGGGTTCAC-3' for PDK3; 5'-GATTGGCTCCTTCTCTGTGG-3' and 5'-TCAAAGGACTTGCCCAGTTT-3' for GLUT1; 5'-GTACCATGCGGAGACCATCA-3' and 5'-GTAGGCGTTATCCAGCGTGA-3' for PKM2; 5'-GCACTCTTCCAGCCTTCCTTCC-3' and 5'-GAGCCGCCGATCCACACG-3' for β-actin.

MTT assay

Cell viability of GBMs was evaluated with the *In vitro* Cell Proliferation Kit 1 (Roche, Mannheim, Germany), which is based on the 3-(4,5-dimethythiazol-2-yl)-2,5-diphenyl tetrazolium bromide (MTT) reduction assay. U251, GBM28, and GBM37 were seeded at a density of 1×10^4 cells/well in 96-well plates and incubated overnight in a 5% CO_2 incubator to ensure cell attachment. Then, cells were treated with DCA at 5, 10, or 20 mM or chrysin at 10, 50, or 100 μM and put in a hypoxia or normoxia incubator for 48 h. After the treatment, 10 μl of MTT (5 μg/ml) was added to each well and the plates were incubated for 4 h at 37°C. Then, 100 μl of solubilization buffer (SDS 10% in 0.01 N HCl) was added to each well of the plates, and the plates were incubated at 37°C overnight. The color was detected spectrophotometrically at 570 nm by a Multiscan MS spectrophotometer (Labsystems, Stockholm, Sweden). DCA and chrysin were purchased from Sigma-Aldrich (St. Louis, MO, USA). All experiments were conducted in triplicate, and these were repeated twice.

Mitochondrial isolation

Mitochondria were isolated as described previously with minor modifications [27]. Cells were harvested by centrifugation at 1,500 g for 5 min. After decanting the supernatant, cells were resuspended in 10 mM of ice-cold Tris buffer (pH 7.6) containing protease inhibitor cocktail (Roche, Mannheim, Germany). Cells were then disrupted mechanically by passing through a 1 ml syringe with a 21-gauge needle 20 times and chemically by the addition of 1.5 M ice-cold sucrose. Subsequently, the disrupted cells were centrifuged at 700 g for 10 min at 2°C. The supernatant containing mitochondria was collected and recentrifuged at 14,000 g for 10 min at 2°C. The resulting pellet was washed and resuspended in 100 μl of 10 mM ice-cold Tris buffer (pH 7.6) containing protease inhibitor cocktail. The 10 μl of isolated mitochondria was taken and lysed for the quantification of protein concentration, and the remaining volumes were stored on ice until functional analysis of mitochondrial complex activities.

Mitochondrial complex activity assays

Mitochondrial complex I, II, and IV activity assays were carried out as described previously with minor modifications [27-29]. For the complex I activity assay, 1 μg of the mitochondrial fraction was preincubated for 3 min at 37°C in 240 μl of 25 mM potassium phosphate buffer (pH 7.8) containing 1.0 μM antimycin-A, 3.5 g/L BSA, 70 μM decylubiquinone, and 60 μM DCIP. The reaction was started by the addition of 5 μl of 160 mM NADH. The complex activity was measured spectrophotometrically at 600 nm at 30 sec intervals for 5 min at 37°C. After 5 min, 2.5 μl of rotenone in dimethyl sulfoxide was added to the reaction mixture and the absorbance was measured at 600 nm for additional 5 min at 30 sec intervals at 37°C for the control groups.

For the complex II activity assay, 1 μg of the mitochondrial fraction was preincubated for 10 min at 37°C in 240 μl of 80 mM potassium phosphate buffer (pH 7.8) containing 1 μM antimycin-A, 1 g/l BSA, 50 μM decylubiquinone, 60 μM DCIP, 3 μM rotenone, 2 mM EDTA, and 0.2 mM ATP. The reaction was started by the addition of 20 μl of 1.5 M succinate and 0.75 μl of 0.1 M KCN, and the activity was assessed spectrophotometrically at 600 nm at 30 sec intervals for 5 min at 37°C. For the control groups, 5 mM malonate was added to the reaction mixture prior to preincubation along with the mitochondrial sample.

For the complex IV activity assay, 1 μg of the mitochondrial fraction was preincubated for 10 min at 30°C in 240 μl of 30 mM potassium phosphate buffer (pH 7.4) containing 2.5 mM dodecylmaltoside. The reaction was started by the addition of 20 μl of 34 μM ferrocytochrome c. The complex activity was measured spectrophotometrically at 550 nm at 30 sec intervals for 5 min at 30°C. For the control groups, 1 mM KCN was added to the reaction mixture prior to preincubation along with the mitochondrial sample.

The activity of citrate synthase, a tricarboxylic acid (TCA) cycle

enzyme, was used to quantify mitochondrial mass and accordingly normalize the activity of mitochondrial complex enzymes as described previously [27]. For the citrate synthase activity assay, 1 μg of the mitochondrial fraction was preincubated for 5 min at 30°C in 240 μl of 50 mM Tris–HCl buffer (pH 7.5) containing 0.2 mM 5,5′-dithiobis-(2-nitrobenzoic acid) and 0.1 mM acetyl-CoA. The reaction was started by the addition of 2.5 μl of 50 mM oxaloacetate. The activity was measured spectrophotometrically at 412 nm at 30 sec intervals for 5 min at 30°C. For control groups, an equivalent volume of water was added instead of oxaloacetate.

Statistical analysis

Data are expressed as means±S.E.M. Two-sample comparisons were carried out using an unpaired two-tailed Student's *t* test. Multiple comparisons were performed using one-way ANOVA or two-way repeated measures ANOVA followed by *post hoc* test. Statistical analysis was performed with the GraphPad Prism 5 software (GraphPad Software, San Diego, CA, USA), and statistical differences were accepted at the 5% level.

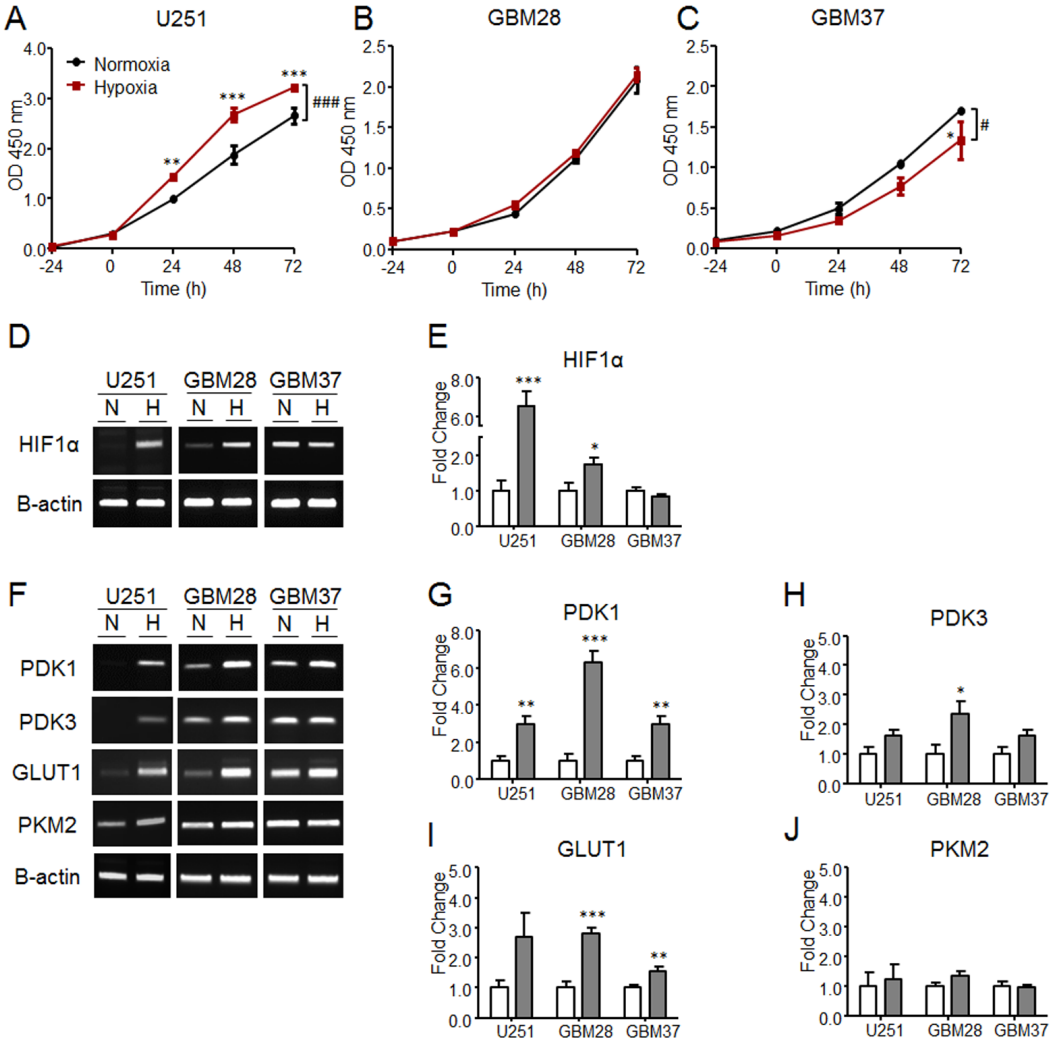

Fig. 1. The cell proliferation rates and the expression levels of hypoxia- and glycolysis-associated genes among different GBM cells under normoxia and hypoxia. (A~C) Growth curves of different GBM cells maintained under normoxic (20% O_2) and hypoxic (1% O_2) conditions. Data are presented as the means±S.E.M (n=8). *, **, and *** denote difference between indicated points at p<0.05, p<0.01, and p<0.001, respectively. #, ##, and ### denote difference between normoxic and hypoxic groups at p<0.05, p<0.01, and p<0.001, respectively (Two-way repeated measures ANOVA followed by *post hoc* test). (D~E) Representative images of RT-PCR (D) and quantified expression levels (E) of HIF1α in GBM cells maintained under normoxic (20% O_2) and hypoxic (1% O_2) conditions for 48 hours. (F~J) Representative images of RT-PCR (F) and quantified expression levels (G~J) of the glycolysis-associated genes, PDK1, PDK3, GLUT1, and PKM2, in GBM cells maintained under normoxic (20% O_2) and hypoxic (1% O_2) conditions for 48 hours. Data are presented as the means±S.E.M (n=4-6 repeats in each group). β-actin was used as an internal control. *, **, and *** denote difference between normoxic and hypoxic groups at p<0.05, p<0.01, and p<0.001, respectively (Student's *t* test).

https://doi.org/10.5607/en.2017.26.5.295

RESULTS

Cell proliferation profiles of GBMs under normoxic and hypoxic conditions

Since hypoxic adaptation is a prominent feature of GBMs [30-32], we first examined the proliferation rates of the GBM cell line U251 and two primary GBMs (GBM28, GBM37) under normoxia (20% O_2) and hypoxia (1% O_2). GBM28 and GBM37 are initial and recurrent tumors, respectively, generated from the same patient. Overall, GBM28 and GBM37 exhibited lower proliferation rates than U251 (Fig. 1A~C). U251 showed significantly higher proliferation rate under hypoxia than normoxia (Fig. 1A). GBM28 showed no difference in growth rates between normoxic and hypoxic conditions (Fig. 1B), which was in contrast to GBM37 exhibiting significantly reduced growth rate under hypoxia compared to that under normoxia (Fig. 1C).

Differential expressions of HIF1α and HIF1α target genes among GBMs under normoxia and hypoxia

Next, we examined the expression level of HIF1α in different GBMs under normoxic and hypoxic conditions. The basal expression level of HIF1α in U251 and GBM28 under normoxia was relatively low, while it was high in GBM37 (Fig. 1D and E). Under hypoxia, the transcript level of HIF1α markedly increased in both U251 and GBM28, whereas it was retained high in GBM37 (Fig. 1D and E). These results indicated that there is a correlation between the increase of proliferation rate and the induction of HIF1α under hypoxia (Fig.1A~E). Then, the expression levels of glycolysis-associated HIF1α target genes were examined. Under normoxia, the basal expression levels of PDK1, PDK3, and GLUT1 were relatively low in U251 and GBM28, while their basal expression levels were high in GBM37 (Fig. 1F~I). Under hypoxia, the expression levels of PDK1, PDK3, and GLUT1 were enhanced further in all GBMs examined, albeit at different levels. The expression levels of PKM2 varied in different GBMs under normoxia and were not altered under hypoxia (Fig. 1F and J). Considering that the overexpression of HIF1α and glycolysis-associated genes has been continuously reported to be correlated with a worse patient outcome [22, 23], greater expression of HIF1α, PDK1, PDK3, and GLUT1 in GBM37 than U251 and GBM28 under normoxia might be a predictable feature of the recurrent tumor.

Inhibition of PDK with DCA induced cell death of GBMs, but the extent of DCA effects varied among cell types

The intervention of glycolytic adaptation with DCA, an inhibitor of PDK, has been reported to offer improved therapeutic outcomes in various tumor types including breast, oral, lung, ovarian, and colon cancers [33-37]. Therefore, we examined the effects of DCA on viabilities of GBM cells cultured under normoxia or hypoxia. The results of MTT assay obtained after 48 h of DCA treat-

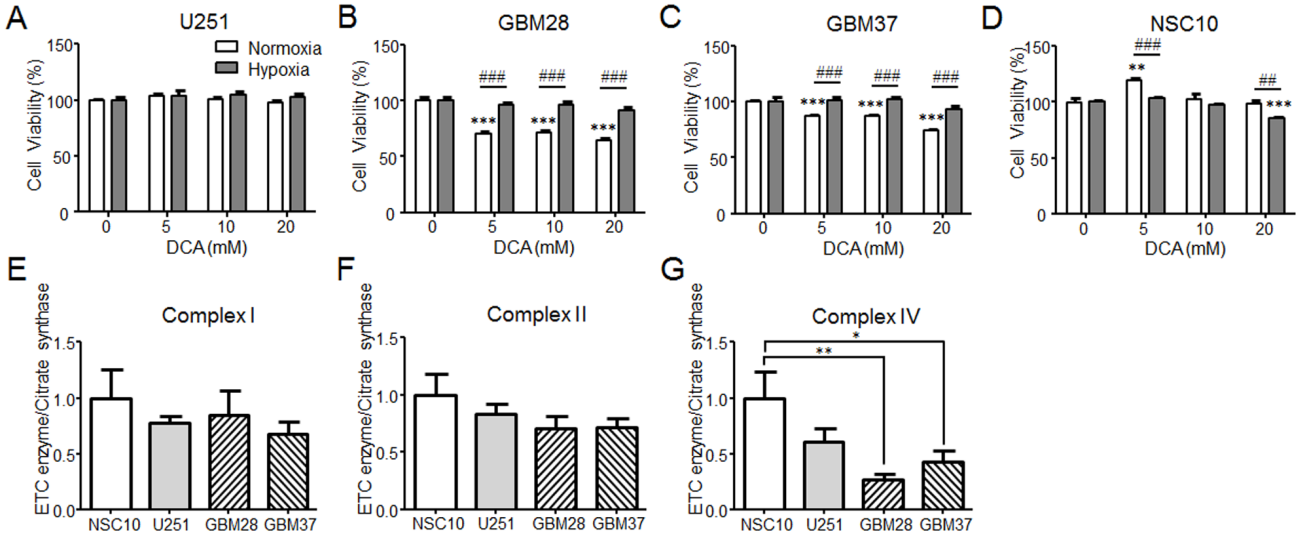

Fig. 2. Inhibition of PDK with DCA induced cell death of GBMs under normoxia, but not under hypoxia. (A~D) Cell viability levels of GBMs (U251, GBM28 and GBM37) and NSC10 in response to different doses (5, 10, or 20 mM) of DCA or vehicle under normoxia (20% O_2) and hypoxia (1% O_2). Cells were treated with indicated doses of DCA for 48 hours. Cell viability levels were measured with the MTT assay. (E~G) Assessments of the mitochondrial complex I (E), II (F), and IV (G) activities in different GBM cells maintained under normoxia (20% O_2). Data are presented as the means±S.E.M ($n \geq 6$). *, **, and *** denote difference between control and indicated point at $p<0.05$, $p<0.01$, and $p<0.001$, respectively. #, ##, and ### denote difference between normoxic and hypoxic groups at $p<0.05$, $p<0.01$, and $p<0.001$, respectively (Student's t test, one-way ANOVA followed by *post hoc* test).

ment indicated that no cell death was induced in U251 at all doses of DCA (5, 10, or 20 mM) under both normoxia and hypoxia (Fig. 2A). Interestingly, in GBM28 and GBM37, DCA treatment at 5, 10, or 20 mM induced significant levels of cell death under normoxia, but DCA at all doses failed to induce cell death under hypoxia (Fig. 2B and C), implying that hypoxic adaptation prevailed DCA effects in these cells. It is notable that DCA treatment in neural stem cells (NSC10) at the dose of 5 or 10 mM did not produce cell death under both normoxic and hypoxic conditions (Fig. 2D), although DCA treatment at 20 mM induced cell death under hypoxia. Overall, these results indicated that DCA effects on inducing cell death under normoxia varied, from no effect in U251 to moderate effects in GBM28 and GBM37, whereas all three GBMs were resistant to DCA treatment under hypoxia.

Reduced utilization of mitochondrial OXPHOS pathway in GBMs

The results of DCA-induced cell death led us to examine the levels of mitochondrial OXPHOS activities in GBMs. The levels of mitochondrial complex I and II activities in U251 were, respectively, 77.1 and 83.5% of the control NSC10, and those in GBM28 and GBM37 were in the range of 67.4 and 85.1% of NSC10 (Fig. 2E and F). The level of mitochondrial complex IV activity in U251 was 60.8% of NSC10, whereas those in GBM28 and GBM37 were,

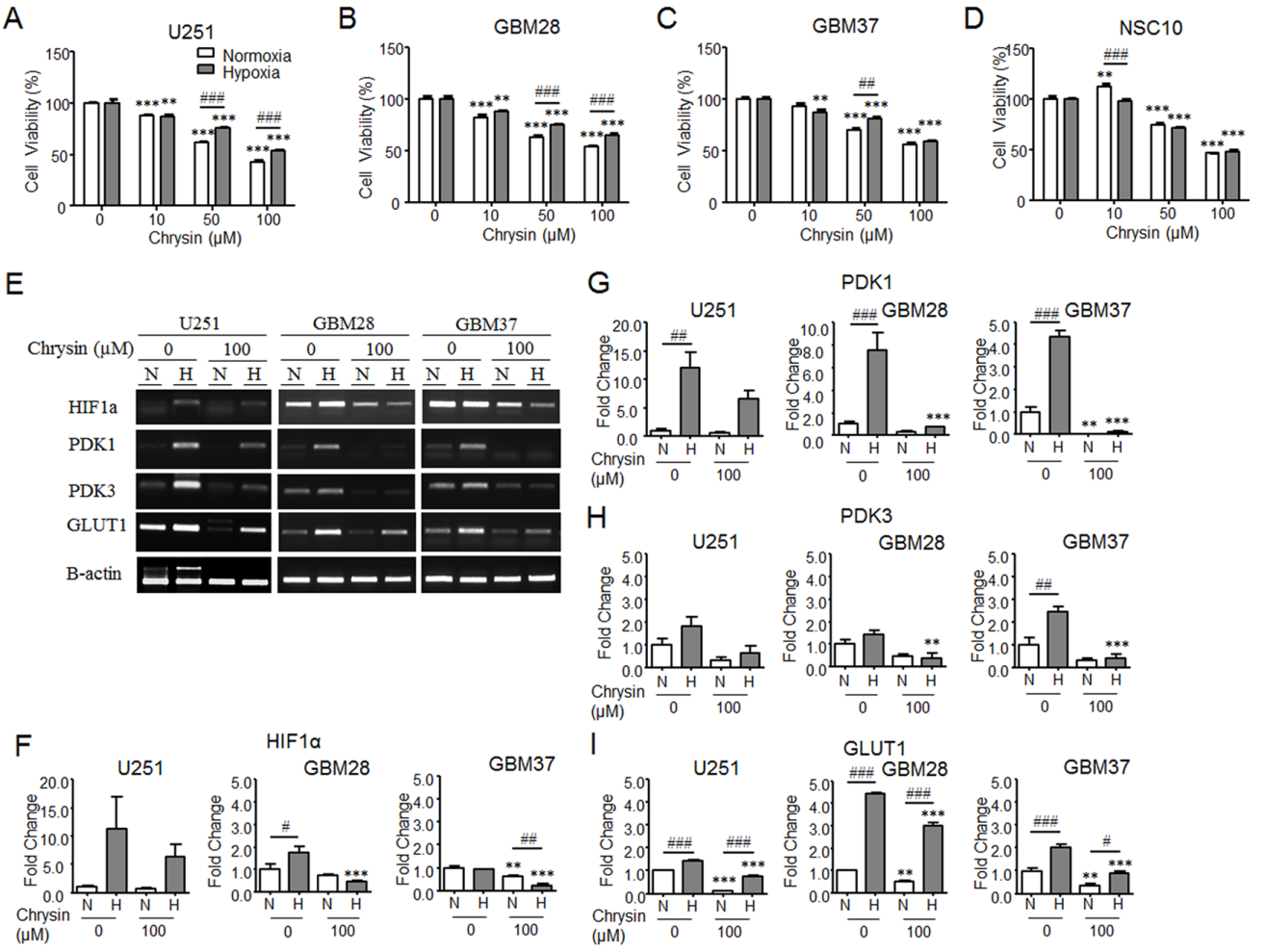

Fig. 3. Inhibition of HIF1α with chrysin induced cell death and suppressed the expressions of glycolysis-regulating genes in GBMs. (A~D) Cell viability levels of GBMs (U251, GBM28 and GBM37) and NSC10 in response to different doses (10, 50, or 100 μM) of chrysin or vehicle under normoxia (20% O_2) and hypoxia (1% O_2). Cells were treated with indicated doses of chrysin for 48 hours. Cell viability levels were measured with the MTT assay. (E~I) Representative images of RT-PCR (E) and quantified expression levels (F~I) of HIF1α, PDK1, PDK3, and GLUT1 in GBM cells treated with chrysin under normoxic (20% O_2) and hypoxic (1% O_2) conditions. Cells were treated with 100 μM of chrysin for 48 hours. Data are presented as the means±S.E.M (n=4 repeats in each group). β-actin was used as an internal control. *, **, and *** denote difference between control and indicated point at $p<0.05$, $p<0.01$, and $p<0.001$, respectively. #, ##, and ### denote difference between normoxic and hypoxic groups at $p<0.05$, $p<0.01$, and $p<0.001$, respectively (Student's *t* test, one-way ANOVA followed by *post hoc* test).

https://doi.org/10.5607/en.2017.26.5.295

respectively, 24.9 and 43.2% of NSC10 (Fig. 2G). These results indicated that the recurrent tumor GBM37 had relatively lower complex I and higher complex IV activities than the initial tumor GBM28 (Fig. 2E and G), and a similar remodeling of mitochondrial complex activities has been reported in a previous report studying TMZ-mediated chemoresistant gliomas [38]. Taken together, these results suggest that compared to NSC10, GBMs had the reduced utilization of OXPHOS pathway and the extent of reduction was prominent for complex IV activity.

Inhibition of HIF1α expression with chrysin induced cell death of GBMs

Next, we examined the physiological significance of hypoxic adaptation in cell viability of GBMs. Treatment of GBMs with chrysin, a naturally occurring flavonoid with an inhibitory activity of HIF1α [39], induced significant levels of cell death in all GBMs under both normoxia and hypoxia (Fig. 3A~C). Although chrysin effects were produced in a dose-dependent manner in all cell types, cells maintained under hypoxia had relatively higher viability than those cultured under normoxia, indicating the continued presence of hypoxia-dependent resistance (Fig. 3A~C). Chrysin treatment suppressed the expressions of HIF1α and the glycolysis-associated genes, PDK1, PDK3, and GLUT1 (Fig. 3E~I). However, the hypoxia-dependent increases of these genes partially remained in all cell types (Fig. 3E~I), which was consistent with chrysin-dependent partial reduction of cell viability of GBMs under hypoxia (Fig. 3A~C). In NSC10, chrysin treatment at 10 μM did not induce cell death under normoxic and hypoxic conditions, whereas chrysin at 50 and 100 μM induced cell death under both normoxic and hypoxic conditions (Fig. 3D). Overall, these results suggest that chrysin induced cell death of all GBMs examined via suppressing the expressions of hypoxia- and glycolysis-associated genes. However, chrysin effects were still weak under hypoxia than those under normoxia, and hypoxia-dependent resistance was sustained in all cell types.

Chrysin-induced cell death was enhanced by the inhibition of PDK in GBMs

Next, we examined whether blocking both hypoxic adaptation and glycolytic adaptation lessened hypoxia-dependent resistance of GBMs. The levels of cell death induced by chrysin at 10 μM increased in all GBMs when DCA at 10 or 20 mM was co-treated (Fig. 4A~C), including U251 which did not respond to DCA alone (Fig. 2A). However, to our surprise, co-treatment of chrysin (10 μM) and DCA (10 or 20 mM) reduced cell viability of NSC10 as well (Fig. 4D), whereas chrysin at 10 μM alone was not toxic to NSC10 (Fig. 3D). When a higher dose of chrysin (100 μM) was co-treated with DCA (10 or 20 mM), cell viability of all GBMs as well

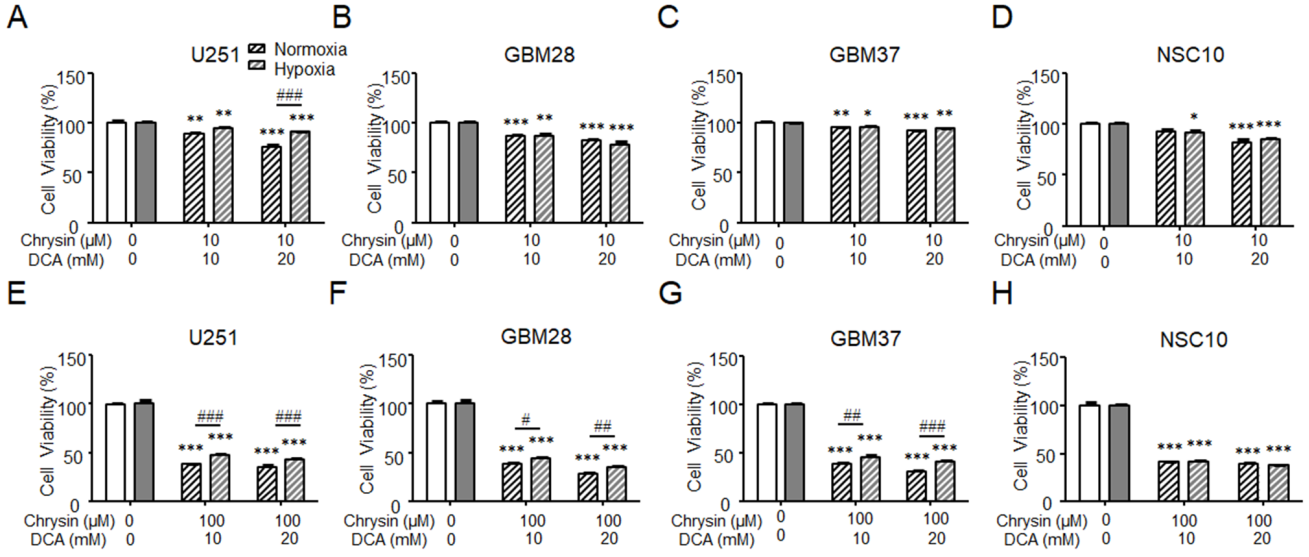

Fig. 4. Co-treatment with chrysin and DCA additively induced cell death of GBMs. (A~D) Cell viability levels of GBMs and NSC10 treated with a combination of chrysin (10 μM) and DCA (10 or 20 mM) under normoxia (20% O_2) and hypoxia (1% O_2). Cells were treated with indicated doses of chrysin and DCA for 48 hours. Cell viability levels were measured with the MTT assay. (E~H) Cell viability levels of GBMs and NSC10 treated with a combination of chrysin (100 μM) and DCA (10 or 20 mM) under normoxia (20% O_2) and hypoxia (1% O_2). Cells were treated as above. Data are presented as the means±S.E.M (n=6). *, **, and *** denote difference between control and indicated point at $p<0.05$, $p<0.01$, and $p<0.001$, respectively. #, ##, and ### denote difference between normoxic and hypoxic groups at $p<0.05$, $p<0.01$, and $p<0.001$, respectively (One-way ANOVA followed by *post hoc* test).

as NSC10 decreased compared to that induced by chrysin (100 μM) alone (Fig. 4E~H). Overall, these results suggest that chrysin and DCA co-treatment produced additive effects on inducing cell death of GBMs. Interestingly however, co-treatment even at high doses of chrysin and DCA was not potent enough to reduce cell viability of GBMs under hypoxia to the levels achieved under normoxia.

DISCUSSION

Mounting evidence has suggested that tumor cells utilize more aerobic glycolysis while using less mitochondrial OXPHOS activity [40, 41]. This metabolic shift becomes enhanced under hypoxia in various tumor cells [21, 42]. Indeed, all GBM cells had reduced oxidative glucose metabolism compared to NSC10, and, in particular, the newly established primary GBMs (GBM28 and GBM37) had significantly reduced mitochondrial complex IV activity compared to NSC10 (Fig. 2E~G). The mitochondrial complex I is the major step where mitochondrial ROS production takes place, and as long as the complex I activity remains low, tumor cells can evade ROS stress resulted from mitochondria [43, 44]. On the other hand, the complex IV is the terminal step of the electron transport chain (ETC), and therefore, the complex IV activity represents the overall ETC activity [38, 45]. The complex I activity in GBM37 tended to be lower than that in GBM28, while the complex IV activity in GBM37 was higher than that in GBM28 (Fig. 2E and G). The reduced demand for aerobic glycolysis in the recurrent tumor GBM37 compared to that in the initial tumor GBM28 might be indicative of reprogrammed tumorigenicity of GBM37 wherein its overall ETC activity in mitochondria was increased [38, 45]. The reduced growth rate of GBM37 under hypoxia (Fig. 1C) might also be related in part to reprogrammed OXPHOS activity. We speculate that GBM37 can maintain its tumorigenicity presumably by regulating both glycolytic and reprogrammed oxidative metabolisms to fit its needs.

PDKs suppress PDH, a mitochondrial enzyme that converts pyruvate into acetyl-CoA to provide the initial substrate for the TCA cycle [46]. U251 was resistant to DCA treatment under normoxia (Fig. 2A), probably because U251 utilized a relatively high level of mitochondrial OXPHOS pathway (Fig. 2E~G). However, as demonstrated in the present study, DCA treatment in GBM28 and GBM37 induced cell death under normoxia, and this DCA effect agrees well with previous reports showing cytotoxic effects of DCA in various tumors including GBMs [8, 34, 47]. DCA-induced cell death of GBM28 under normoxia was slightly higher than that of GBM37 (Fig. 2B and C), which might be correlated with significantly lower expressions of glycolysis-associated genes in GBM28 compared to GBM37 under normoxia (Fig. 1F~J). However, DCA effects on inducing cell death of GBM28 and GBM37 completely disappeared when these cells were cultured under hypoxia, which is considered more physiologically relevant tumor microenvironment than normoxia [25]. These results are consistent in part with

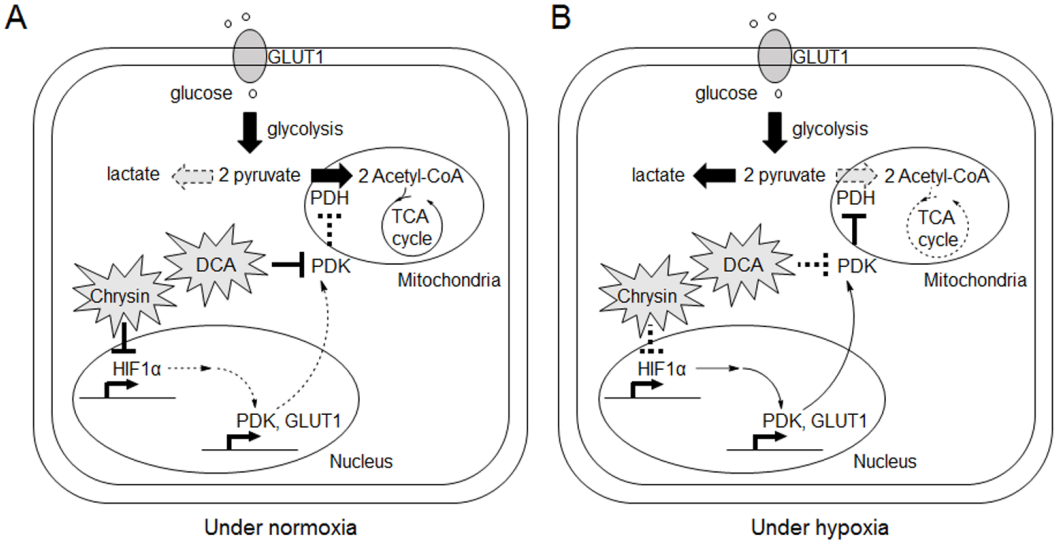

Fig. 5. Schematic diagrams representing chrysin and DCA actions on GBMs. (A) Under normoxia, chrysin treatment suppresses the expression of HIF1α and the HIF1α target genes, GLUT1 and PDKs, and the inhibition of PDKs with DCA disinhibits PDH which provides the initial substrate for the TCA cycle in mitochondria. (B) Under hypoxia, GBMs express high levels of HIF1α and the glycolysis-regulating genes, GLUT1 and PDKs, which promote hypoxia-mediated increase of cell viability along with an increase of glycolytic adaptation. Thus, hypoxia-dependent resistance was sustained in all cell types, and chrysin and DCA co-treatment was ineffective in eliminating this resistance.

https://doi.org/10.5607/en.2017.26.5.295

the increased expression levels of HIF1α and the glycolysis regulating genes, PDK1, PDK3, and GLUT1 in these GBMs under hypoxia (Fig. 1D~I). A similar induction pattern of these genes was detected in U251 maintained under hypoxia, which might contribute to the resistance of this cell line to DCA treatment. Overall, these results suggest that hypoxic adaptation dominates glycolytic adaptation in modulating survival of GBMs, and thus targeting hypoxic adaptation might be more important than intervening glycolytic adaption for treating GBM.

Hypoxia facilitates the metabolic adaptation of cancer cells via HIF1α-dependent regulation of glycolytic genes [22], and the up-regulation of HIF1α is associated with radio- and chemoresistance in GBMs [48, 49]. Our cell viability assay indicated that chrysin treatment produced substantial cell death in all GBMs under normoxia (Fig. 3A~C). Upon chrysin treatment, U251, which was resistant to DCA treatment under normoxia (Fig. 2A), showed cell death to the levels of GBM28 (Fig. 3A and B). Furthermore, chrysin treatment produced cell death in all three GBMs under hypoxia, whereas DCA-induced cell death of these GBMs was absent under hypoxia. These results suggest that chrysin targeted the critical mechanism that controls the viability of GBMs. Similar to the case of DCA-induced cell death, however, GBM37 was still slightly more resistant to chrysin than GBM28 (Fig. 3B and C). For instance, 10 μM of chrysin induced cell death in GBM28 under normoxia but not in GBM37. Chrysin-dependent regulation of HIF1α expression is insufficient to explain the different responses to DCA and chrysin between the initial and recurrent tumors. In addition, considering that chrysin-treated GBM cells under hypoxia still displayed higher viability than those under normoxia, we speculate that chrysin was not potent enough to reduce hypoxia-dependent resistance of GBMs.

Cell death induced by chrysin was further increased when DCA was co-treated (Fig. 4). Co-treatment of chrysin and DCA at low doses (e.g. 10 μM for chrysin and 10 mM for DCA) induced cell death in GBMs under both normoxic and hypoxic conditions, but it is slightly toxic to NSC10 as well (Fig. 4A~D). Chrysin and DCA co-treatment at higher doses also induced cell death in GBMs and NSC10 (Fig. 4E~H). However, it is important to note that hypoxic condition stimulated GBMs to be resistant to both chrysin and DCA treatment, and the co-treatment even with high doses of chrysin and DCA was unable to lessen hypoxia-dependent resilience of GBMs (Fig. 5). Considering these complex results, further detailed studies regarding the mechanisms underlying the resilient response of GBMs to the two treatments under hypoxia should be addressed.

In summary, the inhibition of increased aerobic glycolysis, a metabolic feature of various tumors including GBMs, by DCA produced cell death in GBM28 and GBM37, but not in U251. The inhibition of HIF1α with chrysin, however, pulled down the viability of all three GBMs examined, supporting the possibility that hypoxic adaptation involving HIF1α induction is critical for maintaining cell viability of GBMs. Interestingly, the results of the present study indicated that cell viability of GBMs was still higher under hypoxia than normoxia. Moreover, modulating both glycolytic and hypoxic adaptations by DCA and chrysin, respectively, was ineffective in eliminating this hypoxia-dependent resistance of GBMs, although the co-treatment brought additive effects in inducing cell death. Further extensive studies are necessary to fully elaborate the detailed mechanisms underlying the differential responses of GBMs to DCA and/or chrysin under normoxia and hypoxia.

ACKNOWLEDGEMENTS

This research was supported by the Korea Healthcare Technology R&D Project (grant no. HI11C21100200) of the Ministry of Health & Welfare, Republic of Korea; the Technology Innovation Program (grant no. 10050154, Business Model Development for Personalized Medicine Based on Integrated Genome and Clinical Information) of the Ministry of Trade, Industry & Energy (MI, Korea); the Bio & Medical Technology Development Program of the National Research Foundation (grant no. 2015M3C7A1028926) of the Ministry of Science and ICT, Republic of Korea; and the National Research Foundation of Korea Grant (grant no. NRF-2017M3C7A1047392) of the Ministry of Science and ICT, Republic of Korea.

REFERENCES

1. Parsons DW, Jones S, Zhang X, Lin JC, Leary RJ, Angenendt P, Mankoo P, Carter H, Siu IM, Gallia GL, Olivi A, McLendon R, Rasheed BA, Keir S, Nikolskaya T, Nikolsky Y, Busam DA, Tekleab H, Diaz LA Jr, Hartigan J, Smith DR, Strausberg RL, Marie SK, Shinjo SM, Yan H, Riggins GJ, Bigner DD, Karchin R, Papadopoulos N, Parmigiani G, Vogelstein B, Velculescu VE, Kinzler KW (2008) An integrated genomic analysis of human glioblastoma multiforme. Science 321:1807-1812.
2. Louis DN, Ohgaki H, Wiestler OD, Cavenee WK, Burger PC, Jouvet A, Scheithauer BW, Kleihues P (2007) The 2007 WHO classification of tumours of the central nervous system. Acta Neuropathol 114:97-109.
3. Holland EC (2000) Glioblastoma multiforme: the terminator. Proc Natl Acad Sci U S A 97:6242-6244.
4. Krex D, Klink B, Hartmann C, von Deimling A, Pietsch T,

Simon M, Sabel M, Steinbach JP, Heese O, Reifenberger G, Weller M, Schackert G; German Glioma Network (2007) Long-term survival with glioblastoma multiforme. Brain 130:2596-2606.

5. Stupp R, Mason WP, van den Bent MJ, Weller M, Fisher B, Taphoorn MJ, Belanger K, Brandes AA, Marosi C, Bogdahn U, Curschmann J, Janzer RC, Ludwin SK, Gorlia T, Allgeier A, Lacombe D, Cairncross JG, Eisenhauer E, Mirimanoff RO; European Organisation for Research and Treatment of Cancer Brain Tumor and Radiotherapy Groups; National Cancer Institute of Canada Clinical Trials Group (2005) Radiotherapy plus concomitant and adjuvant temozolomide for glioblastoma. N Engl J Med 352:987-996.
6. Ramirez YP, Weatherbee JL, Wheelhouse RT, Ross AH (2013) Glioblastoma multiforme therapy and mechanisms of resistance. Pharmaceuticals (Basel) 6:1475-1506.
7. Michelakis ED, Sutendra G, Dromparis P, Webster L, Haromy A, Niven E, Maguire C, Gammer TL, Mackey JR, Fulton D, Abdulkarim B, McMurtry MS, Petruk KC (2010) Metabolic modulation of glioblastoma with dichloroacetate. Sci Transl Med 2:31ra34.
8. Li C, Meng G, Su L, Chen A, Xia M, Xu C, Yu D, Jiang A, Wei J (2015) Dichloroacetate blocks aerobic glycolytic adaptation to attenuated measles virus and promotes viral replication leading to enhanced oncolysis in glioblastoma. Oncotarget 6:1544-1555.
9. Solaini G, Sgarbi G, Baracca A (2011) Oxidative phosphorylation in cancer cells. Biochim Biophys Acta 1807:534-542.
10. Kato Y, Ozawa S, Miyamoto C, Maehata Y, Suzuki A, Maeda T, Baba Y (2013) Acidic extracellular microenvironment and cancer. Cancer Cell Int 13:89.
11. Daniele S, Giacomelli C, Zappelli E, Granchi C, Trincavelli ML, Minutolo F, Martini C (2015) Lactate dehydrogenase-A inhibition induces human glioblastoma multiforme stem cell differentiation and death. Sci Rep 5:15556.
12. Velpula KK, Guda MR, Sahu K, Tuszynski J, Asuthkar S, Bach SE, Lathia JD, Tsung AJ (2017) Metabolic targeting of EGFRvIII/PDK1 axis in temozolomide resistant glioblastoma. Oncotarget 8:35639-35655.
13. Stacpoole PW, Kurtz TL, Han Z, Langaee T (2008) Role of dichloroacetate in the treatment of genetic mitochondrial diseases. Adv Drug Deliv Rev 60:1478-1487.
14. Bonnet S, Archer SL, Allalunis-Turner J, Haromy A, Beaulieu C, Thompson R, Lee CT, Lopaschuk GD, Puttagunta L, Bonnet S, Harry G, Hashimoto K, Porter CJ, Andrade MA, Thebaud B, Michelakis ED (2007) A mitochondria-K+ channel axis is suppressed in cancer and its normalization promotes apoptosis and inhibits cancer growth. Cancer Cell 11:37-51.
15. Kluza J, Corazao-Rozas P, Touil Y, Jendoubi M, Maire C, Guerreschi P, Jonneaux A, Ballot C, Balayssac S, Valable S, Corroyer-Dulmont A, Bernaudin M, Malet-Martino M, de Lassalle EM, Maboudou P, Formstecher P, Polakowska R, Mortier L, Marchetti P (2012) Inactivation of the HIF-1α/PDK3 signaling axis drives melanoma toward mitochondrial oxidative metabolism and potentiates the therapeutic activity of pro-oxidants. Cancer Res 72:5035-5047.
16. Liu Z, Chen X, Wang Y, Peng H, Wang Y, Jing Y, Zhang H (2014) PDK4 protein promotes tumorigenesis through activation of cAMP-response element-binding protein (CREB)-Ras homolog enriched in brain (RHEB)-mTORC1 signaling cascade. J Biol Chem 289:29739-29749.
17. Kato M, Li J, Chuang JL, Chuang DT (2007) Distinct structural mechanisms for inhibition of pyruvate dehydrogenase kinase isoforms by AZD7545, dichloroacetate, and radicicol. Structure 15:992-1004.
18. Tatum JL, Kelloff GJ, Gillies RJ, Arbeit JM, Brown JM, Chao KS, Chapman JD, Eckelman WC, Fyles AW, Giaccia AJ, Hill RP, Koch CJ, Krishna MC, Krohn KA, Lewis JS, Mason RP, Melillo G, Padhani AR, Powis G, Rajendran JG, Reba R, Robinson SP, Semenza GL, Swartz HM, Vaupel P, Yang D, Croft B, Hoffman J, Liu G, Stone H, Sullivan D (2006) Hypoxia: importance in tumor biology, noninvasive measurement by imaging, and value of its measurement in the management of cancer therapy. Int J Radiat Biol 82:699-757.
19. Kim Y, Lin Q, Glazer PM, Yun Z (2009) Hypoxic tumor microenvironment and cancer cell differentiation. Curr Mol Med 9:425-434.
20. Shen H, Hau E, Joshi S, Dilda PJ, McDonald KL (2015) Sensitization of glioblastoma cells to irradiation by modulating the glucose metabolism. Mol Cancer Ther 14:1794-1804.
21. Robey IF, Lien AD, Welsh SJ, Baggett BK, Gillies RJ (2005) Hypoxia-inducible factor-1alpha and the glycolytic phenotype in tumors. Neoplasia 7:324-330.
22. Eales KL, Hollinshead KE, Tennant DA (2016) Hypoxia and metabolic adaptation of cancer cells. Oncogenesis 5:e190.
23. Carmeliet P, Dor Y, Herbert JM, Fukumura D, Brusselmans K, Dewerchin M, Neeman M, Bono F, Abramovitch R, Maxwell P, Koch CJ, Ratcliffe P, Moons L, Jain RK, Collen D, Keshert E (1998) Role of HIF-1alpha in hypoxia-mediated apoptosis, cell proliferation and tumour angiogenesis. Nature 394:485-490.
24. Sahlgren C, Gustafsson MV, Jin S, Poellinger L, Lendahl U (2008) Notch signaling mediates hypoxia-induced tumor cell migration and invasion. Proc Natl Acad Sci U S A 105:6392-

6397.
25. McKeown SR (2014) Defining normoxia, physoxia and hypoxia in tumours-implications for treatment response. Br J Radiol 87:20130676.
26. Kang S, Hong J, Lee JM, Moon HE, Jeon B, Choi J, Yoon NA, Paek SH, Roh EJ, Lee CJ, Kang SS (2017) Trifluoperazine, a well-known antipsychotic, inhibits glioblastoma invasion by binding to calmodulin and disinhibiting calcium release channel IP3R. Mol Cancer Ther 16:217-227.
27. Han JY, Kang MJ, Kim KH, Han PL, Kim HS, Ha JY, Son JH (2015) Nitric oxide induction of Parkin translocation in PTEN-induced putative kinase 1 (PINK1) deficiency: functional role of neuronal nitric oxide synthase during mitophagy. J Biol Chem 290:10325-10335.
28. Spinazzi M, Casarin A, Pertegato V, Salviati L, Angelini C (2012) Assessment of mitochondrial respiratory chain enzymatic activities on tissues and cultured cells. Nat Protoc 7:1235-1246.
29. Barrientos A, Fontanesi F, Díaz F (2009) Evaluation of the mitochondrial respiratory chain and oxidative phosphorylation system using polarography and spectrophotometric enzyme assays. Curr Protoc Hum Genet Chapter 19: Unit19.3.
30. Joseph JV, Conroy S, Pavlov K, Sontakke P, Tomar T, Eggens-Meijer E, Balasubramaniyan V, Wagemakers M, den Dunnen WF, Kruyt FA (2015) Hypoxia enhances migration and invasion in glioblastoma by promoting a mesenchymal shift mediated by the HIF1α-ZEB1 axis. Cancer Lett 359:107-116.
31. Wolf A, Agnihotri S, Micallef J, Mukherjee J, Sabha N, Cairns R, Hawkins C, Guha A (2011) Hexokinase 2 is a key mediator of aerobic glycolysis and promotes tumor growth in human glioblastoma multiforme. J Exp Med 208:313-326.
32. Sanzey M, Abdul Rahim SA, Oudin A, Dirkse A, Kaoma T, Vallar L, Herold-Mende C, Bjerkvig R, Golebiewska A, Niclou SP (2015) Comprehensive analysis of glycolytic enzymes as therapeutic targets in the treatment of glioblastoma. PLoS One 10:e0123544.
33. Woo SH, Seo SK, Park Y, Kim EK, Seong MK, Kim HA, Song JY, Hwang SG, Lee JK, Noh WC, Park IC (2016) Dichloroacetate potentiates tamoxifen-induced cell death in breast cancer cells via downregulation of the epidermal growth factor receptor. Oncotarget 7:59809-59819.
34. Ruggieri V, Agriesti F, Scrima R, Laurenzana I, Perrone D, Tataranni T, Mazzoccoli C, Lo Muzio L, Capitanio N, Piccoli C (2015) Dichloroacetate, a selective mitochondria-targeting drug for oral squamous cell carcinoma: a metabolic perspective of treatment. Oncotarget 6:1217-1230.
35. Yang Z, Tam KY (2016) Anti-cancer synergy of dichloroacetate and EGFR tyrosine kinase inhibitors in NSCLC cell lines. Eur J Pharmacol 789:458-467.
36. Li B, Li X, Ni Z, Zhang Y, Zeng Y, Yan X, Huang Y, He J, Lyu X, Wu Y, Wang Y, Zheng Y, He F (2016) Dichloroacetate and metformin synergistically suppress the growth of ovarian cancer cells. Oncotarget 7:59458-59470.
37. Khan A, Andrews D, Blackburn AC (2016) Long-term stabilization of stage 4 colon cancer using sodium dichloroacetate therapy. World J Clin Cases 4:336-343.
38. Oliva CR, Nozell SE, Diers A, McClugage SG 3rd, Sarkaria JN, Markert JM, Darley-Usmar VM, Bailey SM, Gillespie GY, Landar A, Griguer CE (2010) Acquisition of temozolomide chemoresistance in gliomas leads to remodeling of mitochondrial electron transport chain. J Biol Chem 285:39759-39767.
39. Fu B, Xue J, Li Z, Shi X, Jiang BH, Fang J (2007) Chrysin inhibits expression of hypoxia-inducible factor-1alpha through reducing hypoxia-inducible factor-1alpha stability and inhibiting its protein synthesis. Mol Cancer Ther 6:220-226.
40. Marie SK, Shinjo SM (2011) Metabolism and brain cancer. Clinics (Sao Paulo) 66 Suppl 1:33-43.
41. Vander Heiden MG, Cantley LC, Thompson CB (2009) Understanding the Warburg effect: the metabolic requirements of cell proliferation. Science 324:1029-1033.
42. Masoud GN, Li W (2015) HIF-1α pathway: role, regulation and intervention for cancer therapy. Acta Pharm Sin B 5:378-389.
43. Murphy MP (2009) How mitochondria produce reactive oxygen species. Biochem J 417:1-13.
44. Li N, Ragheb K, Lawler G, Sturgis J, Rajwa B, Melendez JA, Robinson JP (2003) Mitochondrial complex I inhibitor rotenone induces apoptosis through enhancing mitochondrial reactive oxygen species production. J Biol Chem 278:8516-8525.
45. Oliva CR, Moellering DR, Gillespie GY, Griguer CE (2011) Acquisition of chemoresistance in gliomas is associated with increased mitochondrial coupling and decreased ROS production. PLoS One 6:e24665.
46. Sutendra G, Michelakis ED (2013) Pyruvate dehydrogenase kinase as a novel therapeutic target in oncology. Front Oncol 3:38.
47. Kinnaird A, Dromparis P, Saleme B, Gurtu V, Watson K, Paulin R, Zervopoulos S, Stenson T, Sutendra G, Pink DB, Carmine-Simmen K, Moore R, Lewis JD, Michelakis ED (2016) Metabolic modulation of clear-cell renal cell carcinoma with dichloroacetate, an inhibitor of pyruvate dehydrogenase kinase. Eur Urol 69:734-744.

48. Chou CW, Wang CC, Wu CP, Lin YJ, Lee YC, Cheng YW, Hsieh CH (2012) Tumor cycling hypoxia induces chemoresistance in glioblastoma multiforme by upregulating the expression and function of ABCB1. Neuro Oncol 14:1227-1238.

49. Hsieh CH, Lee CH, Liang JA, Yu CY, Shyu WC (2010) Cycling hypoxia increases U87 glioma cell radioresistance via ROS induced higher and long-term HIF-1 signal transduction activity. Oncol Rep 24:1629-1636.

https://doi.org/10.5607/en.2017.26.5.295